VOJNOTEHNIČKI GLASNIK/MILITARY TECHNICAL COURIER, 2014., Vol. LXII, No. 2

KINETIC STUDY OF THE CRYSTALLIZATION PROCESS OF THE α-Fe PHASE IN THE AMORPHOUS $Fe_{81}B_{13}Si_4C_2$ ALLOY

Bojan Ž. Janković
University of Belgrade, Faculty of Physical Chemistry, Department of the Dynamics and Structure of Matter, Belgrade, Serbia

DOI: 10.5937/vojtehg62-4586

FIELD: Materials, Chemical Technology
ARTICLE TYPE: Review Paper

Summary:

The kinetic study of the crystallization process of the α-Fe phase from the amorphous $Fe_{81}B_{13}Si_4C_2$ alloy was investigated by DSC and XRD techniques. The kinetic parameters (lnA, E_a) of the investigated process were determined using the Kissinger and isoconversional (model-free) methods. It was established that the α-Fe crystallization process can be described by the JMA (Johnson-Mehl-Avrami) kinetic equation. In accordance with the XRD analysis and the calculated crystallization parameters (n = 4; m = 3), it was concluded that the crystallization stages of the considered process can be described by the bulk nucleation and the three-dimensional (3D) growth of nuclei.

Ključne reči: crystallization; amorphous alloys; kinetic analysis; apparent activation energy; XRD; DSC.

Introduction

Amorphous alloys are relatively new materials offering a specific combination of properties and attracting special interest of many scientists during the last two decades. The amorphous state of matter is, however, structurally and thermodynamically unstable and very susceptible to partial or complete crystallization during thermal treatment or non-isothermal compacting. The crucial limitation with respect to using amorphous alloys for high temperature applications arises from their restricted thermal stability. The onset of exothermic crystallization upon crossing the stability domain of the glassy state results in the formation of highly stable, but brittle intermetallic compounds, which renders these

ACKNOWLEDGEMENTS: This research work was partially supported by the Ministry of Science and Environmental Protection of the Republic of Serbia, under Project 172015.

e-mail: bojanjan@ffh.bg.ac.rs

alloys useful only once. The latter imposes the knowledge of alloys stability in a broad range of temperature due to different crystallization processes, which appears during annealing.

Several techniques have been used to study the crystallization of glasses and amorphous metallic alloys, such as differential scanning calorimetry (DSC) (Yinnon, Uhlmann, 1983, pp.253-75), (de Bruijn, et al., 1981, pp.315), (Vásquez, et al., 2003, pp.153), small angle X-ray scattering (dos Santos, et al., 1997, pp.633-636), electrical resistivity (Jones, et al., 1986, pp.216) and ferromagnetic resonance (Balasubramanian, et al., 1990, pp.1636-1639), (de Biasi, Grillo, 1998, pp.233-236).

Soliman, et al. (Soliman, et al., 2004, pp. 57) investigated the crystallization kinetics of melt-spun $Fe_{83}B_{17}$ metallic glass ribbons. The X-ray diffraction (XRD), scanning electron microscopy (SEM), and differential scanning calorimetry (DSC) were used to investigate the structural and thermal transformations of the $Fe_{83}B_{17}$ metallic glass. The activation energy of the crystallization E_c was evaluated using the different theoretical models, and they obtained the following values of E_c: 235.3, 223.6 and 221.0 kJ mol^{-1}. The same authors applied the modified Johnson-Mehl-Avrami (JMA) equation and they concluded that the $Fe_{83}B_{17}$ crystallization process is governed by a bulk growth in two dimensions (n = 2).

Santos and Santos (dos Santos, dos Santos, 2001, pp.47-52), (dos Santos, dos Santos, 2002, pp.56) investigated the crystallization kinetics of the amorphous alloy Metglass 2605SC ($Fe_{81}B_{13.5}Si_{3.5}C_2$) using the ferromagnetic resonance (FMR), differential scanning calorimetry (DSC) and X-ray diffraction (XRD). Three exothermal peaks can be seen on the presented DSC curves of the investigated alloy, which shows that the crystallization process includes more than one phase. The calculated value of the Avrami exponent for the low temperature DSC peak is n = 1.24, and this value is in good agreement with the FMR results. The obtained results show that the investigated process is diffusion controlled with nucleation rate near zero. The diffraction pattern of Metglass 2605SC shows the amorphous nature of the investigated alloy. The isothermal annealing at T > 780 K leads to the appearance of the crystalline α-Fe and Fe_2B_3 in alloy. The crystallization kinetics of Fe-B-Si metallic glasses ($Fe_{78}B_{13}Si_9$ and $Fe_{81}B_{13.5}Si_{3.5}C_2$) was investigated by X-ray diffraction performed *in-situ* during Joule-heating, with simultaneous monitoring of the electrical resistence and DSC (dos Santos, dos Santos, 2001, pp.47-52), (dos Santos, dos Santos, 2002, pp.56).

The X-ray measurements show that with the increase of annealed temperature of the investigated alloy, the crystallization of the α-Fe and Fe_2B_3 occurs, while at higher temperatures the metastable γ-Fe phase appears. The determined values of the apparent activation energy, E_a (326 and 329 kJ mol^{-1}) for $Fe_{78}B_{13}Si_9$ and 346, 356 and 558 kJ mol^{-1} for

$Fe_{81}B_{13.5}Si_{3.5}C_2$ are comparable with the reported values of E_a for amorphous iron alloys. The values of the Avrami exponent for $Fe_{81}B_{13.5}Si_{3.5}C_2$ at the first and the third peak ($n_{I,III}$ = 1.3) point at the diffusion controlled growth particles of a significant initial volume and the three-dimensional growth of small particles with the zero nucleation rate (dos Santos, dos Santos, 2001, pp.47-52), (dos Santos, dos Santos, 2002, pp.56). The values of the Avrami exponents (n_I = 1.6 and n_{II} = 2.0) calculated for $Fe_{78}B_{13}Si_9$ are characteristical for the diffusion controlled growth of small particles with a decreasing nucleation rate (dos Santos, dos Santos, 2001, pp.47-52), (dos Santos, dos Santos, 2002, pp.56).

Bearing in mind the above exhibited differences in the proposed mechanisms of the α-Fe crystallization from the amorphous alloy and differences in kinetic models and also in the values of kinetic parameters, in this paper, the crystallization process of α-Fe from $Fe_{81}B_{13}Si_4C_2$ alloy was investigated from the kinetic point of view. In order to determine the kinetic triplet for the investigated process, theKissinger peak method (Kissinger, 1957, pp.1702-6) and the Friedman differential isoconversional method (Friedman, 1964, pp.183-195) were applied.

Materials and experimental details

The ribbon-shaped samples of the $Fe_{81}B_{13}Si_4C_2$ amorphous alloy were obtained using the standard procedure of rapid quenching of the melt on a rotating disc (melt-spinning). The obtained ribbon was 2 cm wide and 35 μm thick.

The crystallization process was investigated by differential scanning calorimetry (DSC) in a nitrogen atmosphere using a SHIMADZU DSC-50 analyzer. The sample masses used for DSC measurements were about several miligrams and they were heated in the DSC cell from the room temperature to 650^0C in a stream of nitrogen with N_2 flowing at a rate of 20 mL min^{-1} and at the heating rates of 5, 10, 20 and 30 K min^{-1}.

In order to investigate the structural transformations by X-ray diffraction, the samples of the amorphous alloy $Fe_{81}B_{13}Si_4C_2$ were annealed at different temperatures (298, 473, 573, 673, 823, 873, 973 and 1103 K) in a stream of nitrogen during 30 min. The X-ray powder diffraction (XRD) patterns were recorded on a Philips PW-1710 automated diffractometer using a Cu tube operated at 40 kV and 30 mA. The instrument was equipped with a diffraction beam curved graphite monochromator and the Xe-filled proportional counter. For the routine characterization, the diffraction data were collected in the range of 2θ Bragg angles ($4\text{-}100^0$ counting for 0.1 seconds). For the diffraction data used for crystallite size measurements between $40\text{-}50^0$, the Bragg angles were collected using a four-second scan at 0.02^0 steps, respectively. A fixed 1^0 divergence and 0.1 mm receiving slits

were used. Silicon powder was used as an external standard for the calibration of the diffractometer. All XRD measurements were done with solid samples in the form of ribbon at the ambient temperature.

Microstructural parameters

The crystallite size dimensions (D_{hkl}) were determined by using an interactive Windows program for profile fitting and the size analysis (Winfitt). The full-width at half-maximum (FWHM) values of the peaks at the corresponding Bragg angles were fitted assuming a Pearson VII function for a profile.

Microstrain in the investigated sample was calculated by the following equation:

$$\varepsilon_{hkl} = \frac{\psi}{4tg\theta} \tag{1}$$

where ψ is the width of the diffraction line, which arises only from the structural factors and θ is the Bragg angle.

Methods used to evaluate the crystallization kinetic parameters

Kissinger method

Crystallization kinetics is an important subject in the research of amorphous alloys, and the crystallization apparent activation energy represents the significant part of comprenhensive crystallization kinetics. Usually, the Kissinger equation (Kissinger, 1957, pp.1702-6) is used for the determination of apparent activation energy by measuring crystallization temperatures as a function of heating rates. This method assumes that the reaction rate has a maximum value at the peak temperature (T_p). This assumption also implies a constant degree of conversion (α) at T_p. In many cases, the extent of conversion (α_p) at T_p varies with the heating rate (β). However, in the present study, the analysis of the crystallization data shows that α_p is nearly constant, and we may classify the current method as a special case of the KAS (Kissinger-Akahira-Sunose) isoconversional method. The Kissinger equation (Kissinger, 1957, pp.1702-6) can be presented in the following form as:

$$\ln\left(\frac{\beta}{T_p^2}\right) = \ln\left(\frac{AR}{E_a}\right) - \frac{E_a}{RT_p}, \tag{2}$$

where the plot of $\ln(\beta/T_p^2)$ *versus* $1/T_p$ should give a straight line with the slope, which gives the value of the apparent activation energy (E_a). The pre-exponential factor (A) can be calculated from the intercept value of the estimated straight line.

Isoconversional (model-free) method

The differential isoconversional method was firstly proposed by Friedman (Friedman, 1964, pp.183-195). The basic assumption of the differential isoconversional method is that the reaction rate at a constant conversion value is only a function of temperature. This premise supposes the fact it is accepted to different kinetic parameters, $E_{a,\alpha}$ and A_α, for each value of α over the entire reaction range. The Friedman isoconversional equation can be expressed in the following form:

$$\ln\left[\beta_i\left(\frac{d\alpha}{dT}\right)_{\alpha,i}\right] = \ln\left[A_\alpha f(\alpha)\right] - \frac{E_a}{RT_{\alpha,i}} \tag{3}$$

(henceforth, the subscript α designates the values related to a given conversion, and i is an ordinal number of the non-isothermal experiment conducted at the heating rate β_i). By plotting $\ln[\beta_i(d\alpha/dT)_{\alpha,i}]$ against $1/T_{\alpha,i}$, the value of $-E_a/R$ for a given value of α can be directly obtained. Using this equation, it is possible to obtain the values for E_a over a wide range of conversions.

Results and discussion

Fig. 1 shows the XRD patterns of the $Fe_{81}B_{13}Si_4C_2$ amorphous ribbon which was annealed at different isothermal temperatures (298 K (1), 473 K (2), 573K (3), 673 K (4), 823 K (5), 873 K (6), 973 K (7) and 1103 K (8)).

At the presented diffractogram of the non-annealed $Fe_{81}B_{13}Si_4C_2$ alloy (298 K), a broad peak with the maximum at $2\theta \approx 46.8^0$, characteristic for amorphous materials, can be observed. The annealing of the sample at T = 473 K leads to the appearance of a quite sharp peak at $2\theta \approx 83.8^0$ (Fig. 1). The increase of annealing temperature in the range of 473 K ≤ T ≤ 823 K does not lead to considerable changes in the form of diffractograms, except for the decrease in intensity (a.u.) of the peak at $2\theta \approx 83.8^0$.

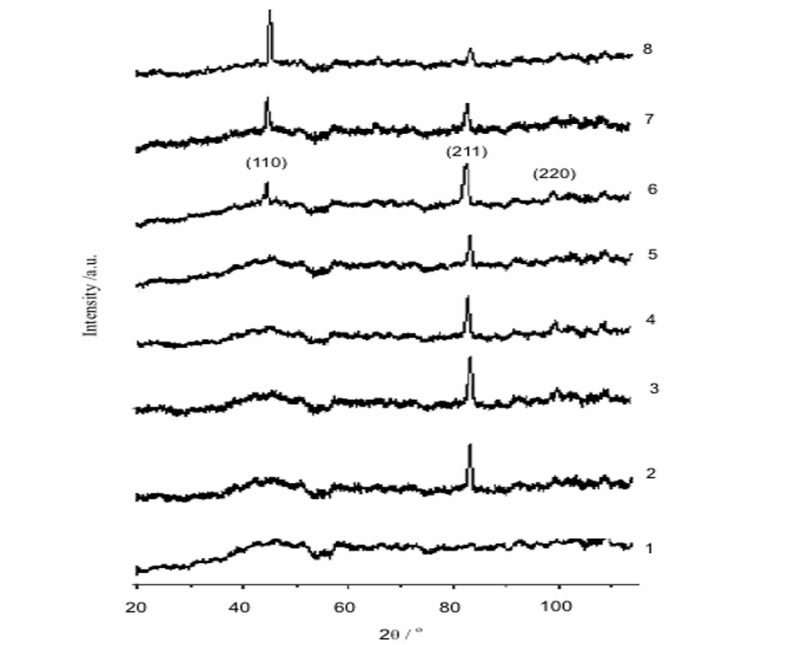

Figure 1 – XRD patterns of the amorphous $Fe_{81}B_{13}Si_4C_2$ alloy in different states, annealed at: 1) 298 K (normal non-annealed state), 2) 473 K, 3) 573 K, 4) 673 K, 5) 823 K, 6) 873 K, 7) 973 K and 8) 1103 K

Slika 1 – XRD prikazi amorfne $Fe_{81}B_{13}Si_4C_2$ legure u različitim stanjima, odgrevane na: 1) 298 K (normalno neodgrevano stanje), 2) 473 K, 3) 573 K, 4) 673 K, 5) 823 K, 6) 873 K, 7) 973 K i 8) 1103 K

In the diffractogram of the annealed alloy at T = 873 K, in respect to the diffractograms of the same alloy annealed at lower temperatures, the appearance of a peak at $2\theta = 46.8^0$ can be observed. Further increase of annealing temperature (873 K ≤ T ≤ 1103 K) leads to the increase in intensity for the peak at $2\theta \approx 46.8^0$ and to the decrease in intensity for the peak at $2\theta \approx 83.8^0$.

The comparative semiquantitative X-ray analysiscan establish that the broad peak at $2\theta \approx 46.8^0$ and the sharp peak at $2\theta \approx 83.8^0$ belong to the α-Fe phase (JPC DS No. 066698).

Bearing in mind the dis-arranged ratio of the intensities of the diffraction lines for the α-Fe phase, the sharp peak at $2\theta \approx 83.8^0$ can be connected with the structurally deformed α-Fe crystalline phase, while the broad peak at $2\theta \approx 46.8^0$ can be connected with the amorphous phase.

If the Scherrer formula for determining the crystallite size was applied on the broad diffraction peak of α-Fe, it can be concluded that in the

non-annealed alloy there are highly disordered clusters of α-Fe, with dimensions of $D_{hkl} \approx 7.1 \times 10^{-10}$ m.

The values of the microstructural parameters of the investigated alloy annealed at different annealing temperatures are presented in Table 1.

The annealing of the alloy at the temperatures $T \leq 973$ K does not lead to significant changes in the microstructure of the formed crystals; however, their relative shares in the annealed alloy decrease. The structurally deformed α-Fe (observed at $T = 473$ K) does not undergo structural changes with the increase of the annealing temperature in the range of 473 K ≤ T ≤ 973 K. The corresponding share of this phase in the alloy increases until a temperature of 823 K, when a newly formed crystal phase appears ($2\theta = 46.8^0$). At $T = 973$ K, the dimensions of crystallites sharply decrease and microstrains in the mentioned crystallites significantly increase.

The microstructural properties of the crystalline α-Fe ($2\theta = 46.8^0$) formed at a temperature of $T = 873$ K from the amorphous clusters of Fe do not change with an increase of the annealing temperature, but their relative share in the sample increases.

Table 1 – Values of the microstructural parameters of $Fe_{81}B_{13}Si_4C_2$ alloy annealed at different temperatures
Tabela 1 – Vrednosti mikrostrukturnih parametara $Fe_{81}B_{13}Si_4C_2$ legure odgrevane na različitim temperaturama

Annealing temperature T /K	$2\theta = 46.8^0$		$2\theta = 83.8^0$	
	$D_{hkl} \times 10^{-10}$ /m	ε_{hkl} /%	$D_{hkl} \times 10^{-10}$ /m	ε_{hkl} /%
473	-	-	139.7	23
573	-	-	139.7	23
673	-	-	139.7	23
823	113	35	139.7	23
873	113	35	139.7	23
973	113	35	139.7	23
1103	113	35	69.9	42

The kinetic study of phase transformations which appear during the procedure of annealing of the $Fe_{81}B_{13}Si_4C_2$ alloy at different temperatures is performed on the basis of the DSC curves recorded at different heating rates. Fig. 2 shows the DSC curves for the $Fe_{81}B_{13}Si_4C_2$ ribbon, recorded at four different heating rates (5, 10, 20 and 30 K min^{-1}).

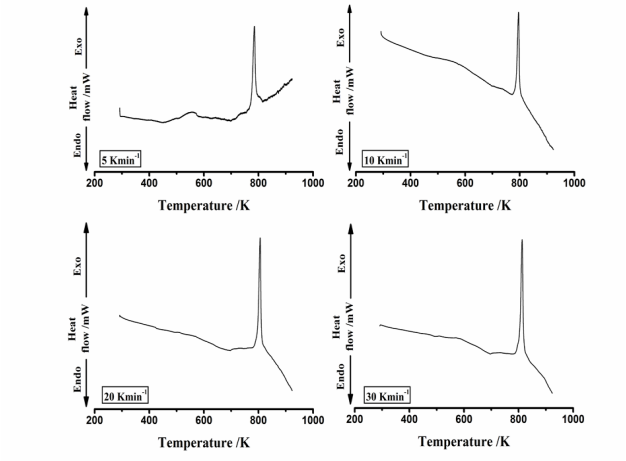

Figure 2 – DSC curves recorded at different heating rates (β = 5, 10, 20 and 30 K min^{-1}) for the amorphous $Fe_{81}B_{13}Si_4C_2$ alloy
Slika 2 – DSC krive snimljene na različitim brzinama zagrevanja (β = 5, 10, 20 and 30 K min^{-1}) za amorfnu $Fe_{81}B_{13}Si_4C_2$ leguru

On all DSC curves, we can see the broad (the low temperature) peak and the sharp (the high temperature) peak. With an increase of the heating rate (β), the values of the initial (T_i), the maximum (T_p) and the final temperature (T_f) for both peaks (Table 2) were shifted to higher values.

Table 2 – The influence of the heating rate (β) on the characteristic temperature values of the DSC curves; The values of the kinetic parameters ($E_{a\ (I;II)}$ and $lnA_{(I;II)}$) calculated by the Kissinger method are given in the same Table.
Tabela 2 – Uticaj brzine zagrevanja (β) na karakteristične temperaturske vrednosti DSC krivih; vrednosti kinetičkih parametara ($E_{a\ (I;II)}$ and $lnA_{(I;II)}$) izračunatih Kisindžerovom metodom prikayane su u istoj tabeli.

β /K min^{-1}	Low temperature peak (I)					High temperature peak (II)				
	T_i /K	T_p /K	T_f /K	$E_{a,I}$ /kJ mol^{-1}	lnA_I	T_i /K	T_p /K	T_f /K	$E_{a,II}$ /kJ mol^{-1}	lnA_{II}
5	450	558	685	134.0	18.12	765	785	815	351.2	52.75
10	460	565	705			774	793	819		
20	465	575	723			782	804	827		
30	472	582	732			786	811	833		

The volume fraction (the degree of conversion) (α) of the sample transformed into the crystalline phase during the crystallization event has been obtained from the DSC curve as a function of the temperature (T). The volume fraction crystallized, α, at any temperature T is given as α =

S_T/S, where S is the total area of the exotherm between the temperature T_i, where the crystallization is just beginning and the temperature T_f, where the crystallization is completed, and S_T is the area between the initial temperature and a generic temperature, T, ranging between T_i and T_f.

The crystallization process which includes the nucleation and growth stages in accordance with the Johnson-Mehl-Avrami (JMA) model (Johnson, Mehl, 1939, pp.416), (Avrami, 1939, pp.1103), (Avrami, 1940, pp.212), (Avrami, 1941, pp.177) can be described by the following equation:

$$\ln\left[-\ln\left(1-\alpha\right)\right] = Const. - n\ln\beta \tag{4}$$

where n is the Avrami kinetic exponent which depends on the mechanism and dimensionality of nucleation and growth.

Fig. 3 shows the relation between ln[-ln(1-α)] and –lnβ (β – is the particular heating rate value) for three fixed temperatures (T = 791, 793 and 795 K) (Eq. (4)).

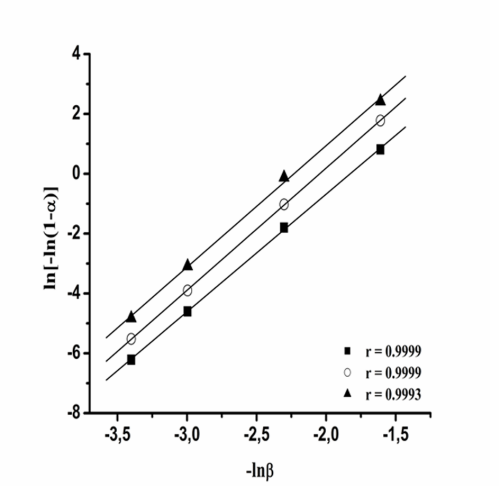

Figure 3 – Plots of ln[-ln(1-α)] versus –lnβ (β in K min^{-1}) at: (■) 791 K; (○) 793 K and (▲) 795 K
Slika 3 – Prave ln[-ln(1-α)] nasuprot –lnβ (β u K min^{-1}) na: (■) 791 K; (○) 793 K i (▲) 795 K

From the presented figure (see Fig. 3), the kinetic (Avrami) exponent n, can be calculated using the linear regression (LR) fitting procedure.

The dependence of ln[-ln(1-α)] *versus* –lnβ at different temperatures (T) shows high values of the linear correlation coefficient (r). The values of n obtained from the slopes of the linear plots presented in Fig. 3, for the considered crystallization process, are given in Table 3.

Table 3 – The changes of the n values with temperature, for the investigated crystallization process of the amorphous $Fe_{81}B_{13}Si_4C_2$ alloy
Tabela 3 – Promene vrednosti n sa temperaturom, za ispitivani proces kristalizacije amorfne $Fe_{81}B_{13}Si_4C_2$ legure

Temperature/K	*n*
791	3.92
793	4.08
795	4.07
Average	4.00

At all considered temperatures, the values of *n*, in the limits of the experimental errors, were approximately the same ($n \approx 4.00$). From these results follows that the kinetics of the crystallization process is independent of the temperature and also, in accordance with Henderson (Henderson, 1979a, pp.325-331), (Henderson, 1979b, pp.301), the above results indicate that the nucleation process occurs with a constant rate.

The Kissinger method is used for the determination of the kinetic parameter values (E_a and ln$A$) for both phase transformations. The Kissinger plots ($\ln(\beta/T_p^2)$ *versus* $1/T_p$) for both considered phase transformations are shown in Fig. 4 (a) and (b).

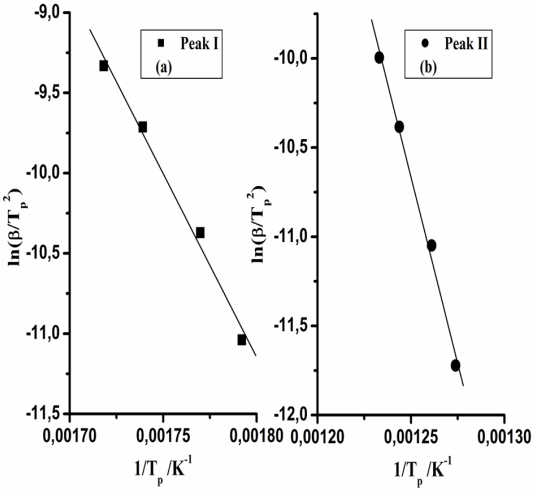

Figure 4 – The Kissinger plots for the low (symbol ■) and high (symbol ●) temperature peak (I (a) and II (b)) at different heating rates, for the considered crystallization process of the amorphous $Fe_{81}B_{13}Si_4C_2$ alloy
Slika 4 – Kisindžerove prave za nisko temperaturni (simbol ■) i visoko temperaturni (simbol ●) pik I (a) i II (b)) na različitim brzinama zagrevanja, za razmatrani proces kristalizacije amorfne $Fe_{81}B_{13}Si_4C_2$ legure

From the slope and the intercept of the linear dependence $\ln(\beta/T_p^2)$ *versus* $1/T_p$, the values of the kinetic parameters (E_a and $\ln A$) are calculated, and the results are presented in Table 2 (columns 5, 6, 10 and 11 in Table 2).

In the case of continuous heating, it can be shown that a generalization of the JMA theory leads to the validation of the Kissinger analysis, through the following equation (Vázquez, et al., 1990, pp.181):

$$n = \left(\frac{d\alpha}{dt}\right)_p RT_p^2 \left(0.37\beta E_a\right)^{-1}, \tag{5}$$

where β is the heating rate, while $(d\alpha/dt)_p$ represents the crystallization rate at the maximum value, i.e., the rate at the peak of an exothermal reaction, detected by the DSC technique. Eq. (5) was derived assuming that usually $E_a >> RT_p$ and that the crystallized fraction, for the maximum crystallization rate is 0.63 (Bezjak, et al., 2007, pp.1), which is independent of the heating rate and of the Avrami kinetic exponent (Vázquez, et al., 1990, pp.181). From the relation $\alpha = S_T/S$, it could be possible to calculate the crystallization rate function, $d\alpha/dt$. Eq. (5) can then be used to determine the Avrami kinetic exponent, n, as an average of the set of parameters obtained for different heating rates.

The values of the Avrami kinetic exponent for the high temperature peak (Table 2) were calculated using Eq. (5). The following values of n were obtained as: n = 3.55, 4.23, 4.00 and 3.68 for β = 5, 10, 20 and 30 K min^{-1}, respectively. If we compare the average value of n evaluated from Eq. (5) ($n_{av} \approx 3.90$), with an average value of n calculated using Eq. (4) for three selected and fixed temperatures ($n_{av} \approx 4.00$, see Table 3), we can conclude that a good agreement exists between these two values.

By the comparison of the results obtained from the X-ray analysis and the DSC measurements, it can be concluded that the sharp X-ray peak positioned at $2\theta \approx 83.8^0$ can be attributed to the processes of rearrangement of the α-Fe clusters, while the peak positioned at $2\theta \approx 46.8^0$ can be attributed to the processes of the α-Fe crystallization, during alloy annealing at certain temperature.

In order to determine the influence of nucleation and crystal growth processes on the values of kinetic parameters, the differential isoconversional (model-free) method was applied, and the corresponding dependence of E_a on α was established. According to the isoconversional method, the linear relationships of $\ln[\beta_i(d\alpha/dT)_{\alpha,i}]$ *versus* $1/T_{\alpha,i}$ were found for the high temperature DSC peak (Fig. 5). This result describes very well the data obtained from the non-isothermal DSC measurements, in the conversion range (α) of $0.05 \leq \alpha \leq 0.90$.

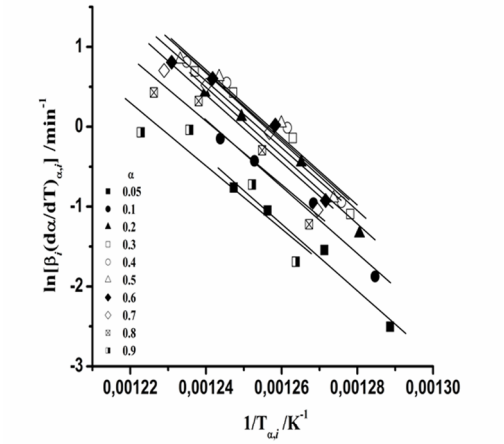

Figure 5 – The dependence of $\ln[\beta_i(d\alpha/dT)_{\alpha,i}]$ versus $(1/T_{\alpha,i})$ at different values of α, for the crystallization process of the amorphous $Fe_{81}B_{13}Si_4C_2$ alloy (full lines are the linear fitting (linearization) corresponding to different α's)
Slika 5 – Zavisnost $\ln[\beta_i(d\alpha/dT)_{\alpha,i}]$ nasuprot $(1/T_{\alpha,i})$ na različitim vrednostima α, za proces kristalizacije amorfne $Fe_{81}B_{13}Si_4C_2$ legure (pune linije su linearno fitovanje ,linearizacija, koje odgovara različitim α)

The values of the apparent activation energy (E_a) and the apparent intercepts ($\ln[A_\alpha f(\alpha)]$) were calculated by means of this method, and the obtained results are presented in Fig. 6. Any point in this figure (corresponding to E_a for constant α) was obtained from Eq. (3), within the certain experimental error limits (specified by the error bars).

The Friedman differential method for the calculation of the apparent activation energy values removes the systematic errors due to the approximation of the temperature integral. However, it can be pointed out that the Friedman method introduces large errors for small values of ($\beta d\alpha/dT$), such as near the onset and sometimes near the end of the reaction (Vyazovkin, Wight, 1998, pp.407), (Munteanu, et al., 2003, pp.1995).

It can be observed that the apparent activation energy for the considered crystallization process is practically constant in $0.05 \leq \alpha \leq 0.90$ range, and its values were found to be $E_a = 347.3 \pm 5.5$ kJ mol^{-1}.

The above results indicate that there is a high probability for the presence of a *single-step reaction* (Vyazovkin, 2000, pp.155), (Opfermann, Flammersheim, 2003, pp.1), i.e., this statement is in agreement with the above exhibited unique process of nucleus growth with a value of $E_{a,G} = 347.3$ kJ mol^{-1} (the average value obtained by the differential isoconversional method). The value of the apparent activation energy calculated by the differential isoconversional method is lower than the value of the apparent activation energy calculated by the Kissinger method ($E_{a,Kissinger} = 351.2$ kJ mol^{-1} (attached to peak II)).

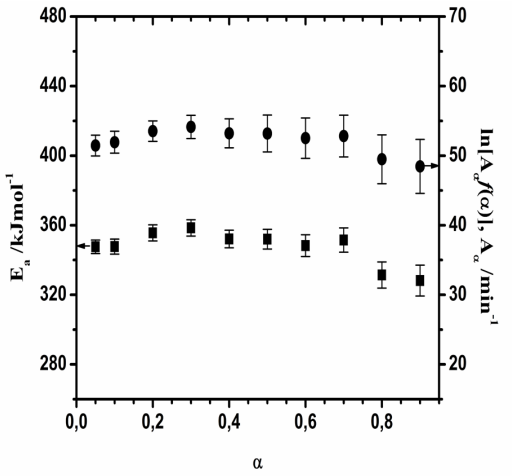

Figure 6 – The apparent activation energy (E_a) (full square symbol) and the apparent intercept ($\ln[A_\alpha f(\alpha)]$) (full circle symbol) values calculated by the Friedman method, plotted as a function of the fractional conversion (α), for the crystallization process of the amorphous $Fe_{81}B_{13}Si_4C_2$ alloy

Slika 6 – Vrednosti prividne energije aktivacije (E_a) (puni kvadratni simboli) i vrednosti prividnih odsečaka ($\ln[A_\alpha f(\alpha)]$) (puni kružni simboli) izračunati Fridmanovom metodom, a predstavljeni u funkciji konverzione frakcije (α), za proces kristalizacije amorfne $Fe_{81}B_{13}Si_4C_2$ legure

Fig. 7 shows the dependence of ln*A* versus α evaluated for the JMA reaction model with $n = 4.0$ (model A4). The values of ln*A* for constant α are calculated by introducing the JMA reaction model (A4) in the Friedman apparent intercepts obtained from Fig. 5 (Eq. (3): $\ln[Af(\alpha)]$).

Fig. 7 shows that the values of ln*A* follows the same trend as the values of the apparent activation energy on the degree of conversion (α) (Fig. 6). This dependence is evaluated for the JMA model function in the form of $f(\alpha) = 4(1 - \alpha)[- \ln(1 - \alpha)]^{3/4}$ at $n = 4.0$.

It can be pointed out that the crystallization exponent *n* is connected with the number of growth dimensions (*m*) and the number of nuclei forming stages (*s*) (Brown, Dollimore, Galwey, 1980) by the following equation:

$$n = m + s, \tag{6}$$

where *m* is the number of growth dimensions ($m = 1$ for one-dimensional growth; $m = 2$ for two-dimensional growth (for disc and cylinder) and $m = 3$ for three-dimensional growth (for sphere and half-sphere)), *s* is the number of the nuclei forming stages ($s = 0$ for the instantaneous nucleation; $s = 1$ for the constant nucleation rate, and $s > 1$ for the self-acceleratory nucleation rate). In order to describe in detail the considered crystallization process, the value of the parameter *m* should be determined.

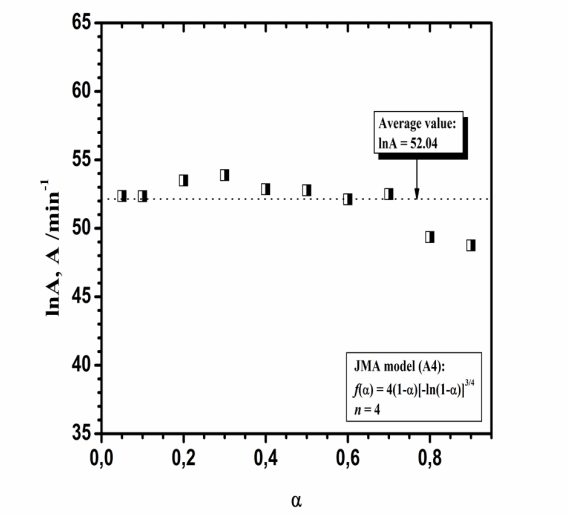

Figure 7 – The logarithm of the pre-exponential factor (lnA) calculated from the differential (Friedman) isoconversional method as a function of the fractional conversion (α) for function $f(\alpha) = 4(1 - \alpha)[- \ln(1 - \alpha)]^{3/4}$ (n = 4.0), in the case of the crystallization process of the amorphous $Fe_{81}B_{13}Si_4C_2$ alloy (the dot line represents the average value of lnA)
Slika 7 – Logaritam predeksponencijalnog faktora (lnA) izračunat iz diferencijalne (Fridman) izokonverzione metode u funkciji konverzione frakcije (α) za funkciju $f(\alpha) = 4(1 - \alpha)[- \ln(1 - \alpha)]^{3/4}$ (n = 4.0), u slučaju procesa kristalizacije amorfne $Fe_{81}B_{13}Si_4C_2$ legure (tačkasta linija predstavlja srednju vrednost lnA)

In accordance with Farjas and Roura (Farjas, Roura, 2006, pp.5573), the fractional extent of the reaction can be expressed as:

$$\alpha = 1 - \exp\left\{ -\left[AC \frac{E_a}{\beta R} p\left(\frac{E_a}{RT} \right) \right]^{m+1} \right\} \tag{7}$$

where E_a represents the overall apparent activation energy ($E_a = (E_{a,N} + m \cdot E_{a,G})/n$), and C is a constant that depends on m, $E_{a,N}$ and $E_{a,G}$

$$C \equiv \left[\frac{(m+1)! E_a^{m+1}}{\prod_{i=0}^{m} (E_{a,N} + i E_{a,G})} \right]^{\frac{1}{m+1}} . \tag{8}$$

The function $p(E_a/RT)$ in Eq. (7) represents the temperature integral, with the reduced apparent activation energy expressed as $x = E_a/RT$.

Taking the double-logarithmic form of Eq. (7), it follows:

$$\ln\left[-\ln(1-\alpha)\right] = (m+1)\ln\left(p\left(\frac{E_a}{RT}\right)\right) + (m+1)\ln\left(AC\frac{E_a}{\beta R}\right) \quad (9)$$

By substituting $p(x)$ by its first-order approximation (Woldt, 1992, pp.521), (Ruitenberg, et al., 2001, pp.97), (Starink, 2003, pp.163) gives:

$$\ln\left[-\ln(1-\alpha)\right] = (m+1)\ln\left[\frac{\exp\left(-\frac{E_a}{RT}\right)}{\left(\frac{E_a}{RT}\right)^2}\right] + (m+1)\ln\left(AC\frac{E_a}{\beta R}\right). \quad (10)$$

It can be easily verified numerically that the plot of $\ln(p(x))$ versus x for $20 < x < 60$ exhibits a clear linear trend as: $\ln(p(x)) \approx -5.2813 - 1.051x$ (Starink, 2003, pp.163). Therefore, Eq. (10) can be reduced to Eq. (11):

$$\ln\left[-\ln(1-\alpha)\right] = -1.051(m+1)\frac{E_a}{RT} + (m+1)\times\ln\left(AC\frac{E_a}{\beta R}\right) - 5.2813 \quad (11)$$

Thus, the plot of ln[-ln(1-α)] as a function of the reciprocal absolute temperature is linear with a slope of $-1.051\times(m+1)E_a/R$.

The straight line dependence between ln[-ln(1-α)] and $(1/T)$ at all considered heating rates was obtained. Based on the above facts, the calculation of the parameter m is possible.

The values of the parameters m and s obtained at different heating rates (β) for the investigated crystallization process of the α-Fe phase, in $Fe_{81}B_{13}Si_4C_2$ amorphous alloy are given in Table 4.

Table 4 – The dependence of the m and s parameter values on the heating rate β, for the crystallization process of the amorphous $Fe_{81}B_{13}Si_4C_2$ alloy
Tabela 4 – Zavisnost vrednosti m i s parametara od brzine zagrevanja β, za proces kristalizacije amorfne $Fe_{81}B_{13}Si_4C_2$ legure.

β /K min^{-1}	*m*	*s*
5	2.84	1.16
10	3.08	0.92
20	3.22	0.78
30	2.84	1.16
Average	3.00	1.00

Based on the obtained values of the parameters *m* and *s*, at different heating rates (Table 4), we can assume that the nucleation process of the α-Fe phase occurs within the amorphous alloy with a constant rate. The growth of α-Fe crystallites occurs in three geometrically effective directions (the three-dimensional (3D) growth) and this process also proceeds with a constant rate.

Conclusion

Bearing in mind all the above exhibit results, we can establish the following conclusions:

i) In the non-annealed sample of the $Fe_{81}B_{13}Si_4C_2$ alloy, there are highly disordered clusters of the α-Fe phase.

ii) The isothermal annealing of the alloy sample at T = 473 K leads to the formation of the structurally deformed crystalline α-Fe phase of nano-dimensions i.e., the simultaneous existing of the amorphous non-crystalline α-Fe phase in the sample.

iii) Further crystallization of α-Fe in the considered alloy at a higher annealing temperature precedently follows the phase transformation within the α-Fe cluster by a disorder-order type with $E_{a,I}$ =134.0 kJ mol^{-1} and lnA_I = 18.12.

iv) The isothermal crystallization was governed on the previously formed nucleuses of the α-Fe phase, with the three-dimensional (3D) growth of α-Fe crystal germs.

v) The kinetics of the non-isothermal crystallization was described by the JMA (Johnson-Mehl-Avrami) equation with the following values of the kinetic parameters: m = 3.0, s = 1.0 (n = 4.0) and E_a = 347.3 kJ mol^{-1}.

vi) At T > 973 K, the structurally deformed crystalline phase of α-Fe was dissolved and it participated in the crystal growth of the crystalline α-Fe.

The obtained DSC (the two peaks were found – peak I and II), the XRD results, and in addition, the kinetic description of the crystallization process are contrary to the results obtained by the Santos and Santos (dos Santos, dos Santos, 2001, pp.47-52), (dos Santos, dos Santos, 2002, pp.56). These facts point to the physico-chemical and microstructural differences between the investigated samples, which are caused by the different procedures of their preparation.

Literature

Avrami, M. 1939. . *J. Chem. Phys.,* 7, p 1103.

Avrami, M. 1940. . *J. Chem. Phys.,* 8, p 212.

Avrami, M. 1941. Granulation, phase change, and microstructure: Kinetics of phase change. III. *Journal of Chemical Physics,* 9(2), p 177. doi:10.1063/1.1750872

Balasubramanian, G., Tiwari, A.N., & Srivastava, C.M. 1990. Applicability of FMR for crystallization studies in metallic glasses. *Journal of Materials Science,* 25(3), pp. 1636-1639. doi:10.1007/BF01045363

Bezjak, A., Kurajica, S., & Šipušić, J. 2007. . *Croat. Chem. Acta,* 80, p 1.

Brown, W.E., Dollimore, D., & Galwey, A.K. 1980. *Reactions in the solid state*. Amsterdam: Elsevier.

de Biasi, R.S., & Grillo, M.L.N. 1998. . *J. Alloys Comp.,* 279, pp. 233-236.

de Bruijn, T.J.W., de Jong, W.A., & van den Berg, P.J. 1981. . *Thermochim. Acta,* 45, p 315.

dos Santos, D.R., Torriani, I.L., Ramos, A.Y., & Knobel, M. 1997. Small-Angle X-ray Scattering Study of Nanocrystalline and Amorphous States of the Fe73.5CuNb3Si13.5B9 Alloy. *Journal of Applied Crystallography,*30(5), pp. 633-636. doi:10.1107/S0021889897001891

dos Santos, D.R., & dos Santos, D.S. 2001. . *Mater. Res.,* 4, pp 47-52.

dos Santos, D.S., & dos Santos, D. 2002. . *Journal of Non-Crystalline Solids,* 304(1-3), p 56. doi:10.1016/S0022-3093(02)01004-9

Farjas, J., & Roura, P. 2006. . *Acta Materialia,* 54, p 5573.

Friedman, H.L. 1964. Kinetics of thermal degradation of charforming plastics from thermogravimetry. Application to a phenolic plastic. *J. Polym. Sci.,* 6, pp 183-195.

Henderson, D.W. 1979a. Experimental analysis of non-isothermal transformations involving nucleation and growth. *Journal of Thermal Analysis,* 15(2), pp 325-331. doi:10.1007/BF01903656

Henderson, D.W. 1979b . *J. Non-Cryst. Solids,* 30, p 301.

Johnson, W.A., & Mehl, R.F. 1939. . *Trans. Amer. Inst. Min. Metal. Petro. Eng,* 135, p 416.

Jones, G.A., Bonnett, P., & Parker, S.F.H. 1986. . *J. Magn. Magn. Mater,* 58, p 216.

Kissinger, H.E. 1957. Reaction kinetics in differential thermal analysis. *Anal. Chem. ,* 29, pp 1702-6. doi:10.1021/ac60131a045

Munteanu, G., Budrugeac, P., Ilieva, L., Tabakova, T., Andreeva, D., & Segal, E. 2003. . *J. Mater. Sci.,* 38, p 1995.

Opfermann, J.R., & Flammersheim, H.J. 2003. . *Thermochim. Acta,* 397, p 1. doi:10.1016/S0040-6031(02)00169-7

Ruitenberg, G., Woldt, E., & Petford-Long, A.K. 2001. . *Thermochim. Acta,* 378, p 97.

Soliman, A.A., Al-Heniti, S., Al-Hajry, A., Al-Assiri, M., & Al-Barakati, G. 2004. . *Thermochim. Acta,* 413, p 57.

Starink, M.J. 2003. . *Thermochim. Acta,* 404, p 163.

Vázquez, J., Ligero, R.A., Villares, P., & Jiménez-Garay, R. 1990. . *Thermochim. Acta,* 157, p 181.

Vásquez, J., López-Alemany, P.L., Villares, P., & Jiménez-Garay, R. 2003. . *J Alloys Comp.,* 354, p 153.

Vyazovkin, S. 2000. . *Thermochim. Acta,* 355, p 155.

Vyazovkin, S., & Wight, C.A. 1998. . *Int. Rev. Phys. Chem,* 17, p 407.

Woldt, E. 1992. . *J. Phys. Chem. Solids,* 53, p 521.

Yinnon, H., & Uhlmann, D.R. 1983. Applications of thermoanalytical techniques to the study of crystallization kinetics in glass-forming liquids, Part I: Theory. *Journal of Non-Crystalline Solids,* 54(3), pp. 253-75. doi:10.1016/0022-3093(83)90069-8

KINETIČKO ISPITIVANJE PROCESA KRISTALIZACIJE α-Fe FAZE IZ AMORFNE LEGURE $Fe_{81}B_{13}Si_4C_2$

OBLAST: materijali, hemijske tehnologije
VRSTA ČLANKA: pregledni članak

Sažetak:

Kinetičko ispitivanje procesa kristalizacije α-Fe faze iz amorfne legure $Fe_{81}B_{13}Si_4C_2$ ispitan je pomoću DSC i KSRD tehnike. Kinetički parametri (LNA, Ea) kod ispitivanih procesa određeni su korišćenjem Kisindžer metode i "isoconversional" metode. Utvrđeno je da se α-Fe proces kristalizacije može opisati JMA (Johnson-Mehl-Avrami) kinetičkom jednačinom. U skladu sa KSRD analizom i izračunatim parametrima kristalizacije (n = 4, m = 3), zaključeno je da se faze procesa kristalizacije mogu opisati rasutom nukleacijom i trodimenzionalnim (3D) rastom jezgara.

Ključne reči: *kristalizacija, amorfne legure, kinetička analiza, prividna energija aktivacije, XRD, DSC.*

Datum prijema članka/Paper received on: 04. 10. 2013.
Datum dostavljanja ispravki rukopisa/Manuscript corrections submitted on: 20. 12. 2013.
Datum konačnog prihvatanja članka za objavljivanje/ Paper accepted for publishing on: 22. 12. 2013.